JOURNAL OF CHEMICAL INFORMATION AND MODELING

Article

pubs.acs.org/jcim

# Identification of a New Class of FtsZ Inhibitors by Structure-Based Design and *in Vitro* Screening

Fung-Yi Chan,[†,‡] Ning Sun,[†] Marco A. C. Neves,[‡] Polo Chun-Hung Lam,[§] Wai-Hong Chung,[†] Lai-King Wong,[†] Ho-Yin Chow,[†] Dik-Lung Ma,[†] Pak-Ho Chan,[†] Yun-Chung Leung,[†] Tak-Hang Chan,[†] Ruben Abagyan,[‡,§] and Kwok-Yin Wong*[,†]

[†]Department of Applied Biology and Chemical Technology and State Key Laboratory of Chirosciences, The Hong Kong Polytechnic University, Hung Hom, Kowloon, Hong Kong, P. R. China

[‡]Skaggs School of Pharmacy and Pharmaceutical Sciences, University of California, San Diego, 9500 Gilman Drive, MC 0747 La Jolla, California 92093-0747, United States

[§]Molsoft L.L.C, 11199 Sorrento Valley Road, S209, San Diego, California 92121, United States

Supporting Information

**ABSTRACT:** The Filamenting temperature-sensitive mutant Z (FtsZ), an essential GTPase in bacterial cell division, is highly conserved among Gram-positive and Gram-negative bacteria and thus considered an attractive target to treat antibiotic-resistant bacterial infections. In this study, a new class of FtsZ inhibitors bearing the pyrimidine-quinuclidine scaffold was identified from structure-based virtual screening of natural product libraries. Iterative rounds of *in silico* studies and biological evaluation established the preliminary structure−activity relationships of the new compounds. Potent FtsZ inhibitors with low micromolar $IC_{50}$ and antibacterial activity against *S. aureus* and *E. coli* were found. These findings support the use of virtual screening and structure-based design for the rational development of new antibacterial agents with innovative mechanisms of action.

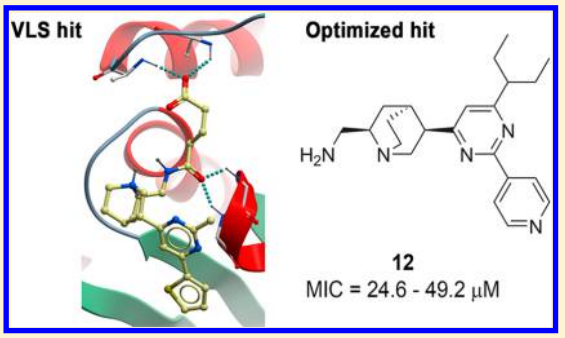


## INTRODUCTION

Antimicrobial resistance is a global threat to public health that greatly increases the costs for treatment of bacterial infections and reduces the efficacy of widely prescribed antibiotics against bacterial strains such as methicillin-resistant *Staphylococcus aureus* (MRSA) and vancomycin-resistant *Enterococcus faecium*.[1,2] Aggressive bacteria with resistance to drugs of last resort such as carbapemens, fluoroquinolones, and vancomycin have emerged in the past decade.[3] Because the infections by antibiotic-resistant bacteria are responsible for higher morbidity and mortality rates than similar infections by antibiotic-susceptible strains, new antibacterial agents with innovative mechanisms of action are urgently needed.[4]

Filamenting temperature-sensitive mutant Z (FtsZ), a prokaryotic homologue of the eukaryotic cytoskeleton tubulin,[5] plays a critical role in bacterial cell division and is highly conserved in a wide range of bacteria.[6−8] During bacterial cytokinesis, FtsZ assembles into a highly dynamic cytoskeleton scaffold (the Z-ring) by undergoing GTP-dependent polymerization, generating protofilaments at the site of septum formation.[9,10] Subsequently, FtsZ recruits other downstream proteins responsible for the invagination of cell membrane and septum formation, completing the bacterial cell division.[11,12] Bacterial cell division proteins such as FtsZ have thus been recognized as attractive targets for the development new antibacterial agents.[13,14] To date, a number of compounds have already been shown to inhibit bacterial growth through the interference with GTP hydrolysis or/and dynamic assembly of cell division protein FtsZ.[15−20] Totarol, a phenolic diterpenoid produced by many plants, was reported to be effective against Gram-positive bacteria by inhibiting the GTPase activity of FtsZ.[21] Chrysophaentin A, isolated from marine sources, was shown to perturb the functional activity of FtsZ in clinically relevant Gram-positive bacteria.[22] Alkyoxybenzamide derivatives, such as PC190723, showed potent antibacterial activity as well as synergistic effects when combined with $\beta$-lactam antibiotics against an *in vivo* mouse model of methicillin-resistant *Staphylococcus aureus*.[23,24] Despite these encouraging results, the clinical applicability of bacterial cell division inhibitors against antibiotic-resistant bacteria is yet to be demonstrated, and new chemical scaffolds for the design of potent FtsZ inhibitors are still required.

Computer-assisted rational design approaches have been widely used in the early stages of drug discovery.[25,26] In particular, structure-based virtual screening of large natural compound libraries is a popular approach to identify new antibacterial agents.[27,28] Indeed, more than half of the clinically

**Received:** April 5, 2013
**Published:** July 12, 2013

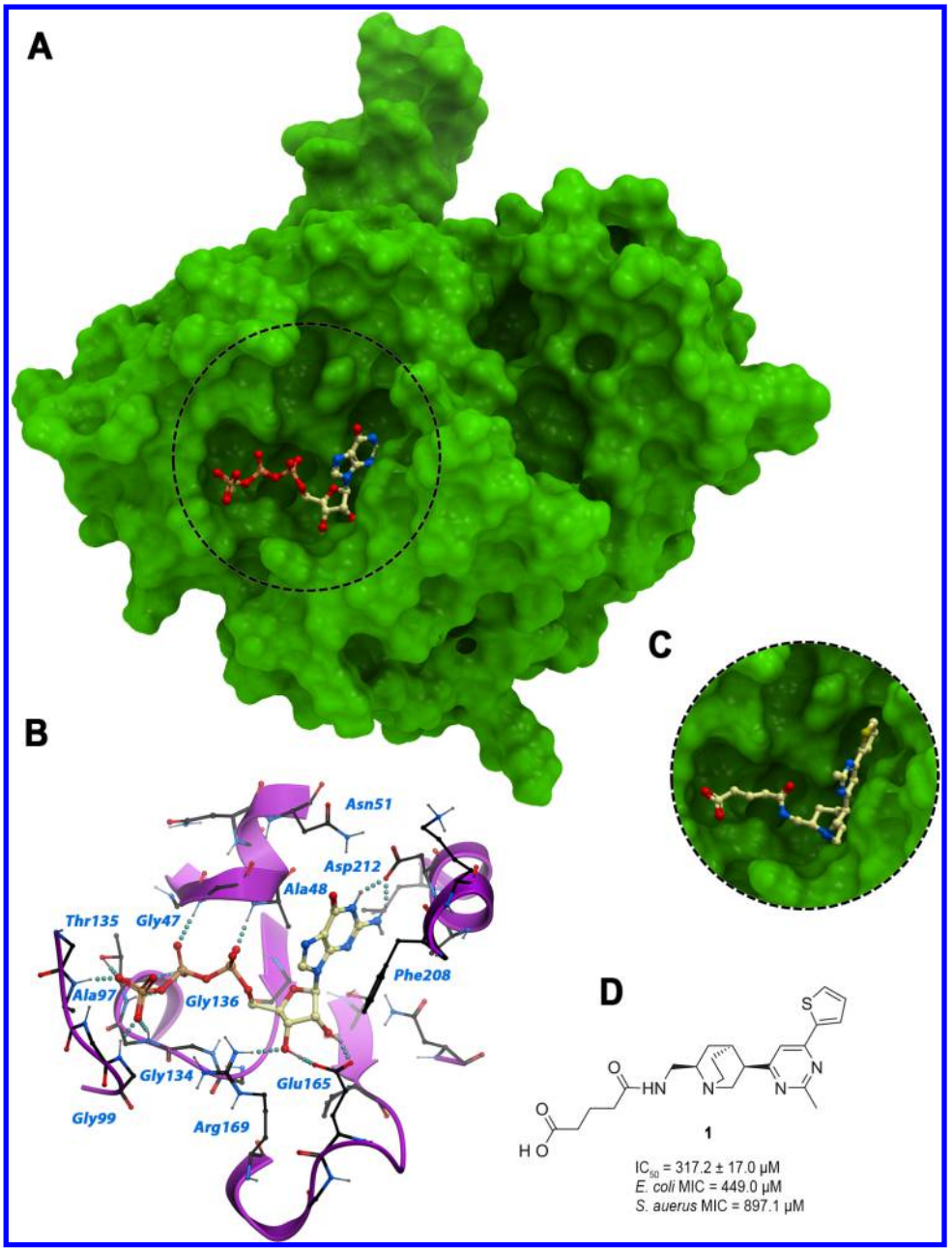


**Figure 1.** The Analyticon Discovery compounds were docked against the X-ray crystal structure of *M. jannaschii* FtsZ (PDB entry 1W5B).[10] A) The GTP binding site is highlighted with a dashed circle, and the GTP cocrystal is represented with a 'ball and sticks' model. B) Details on the GTP binding site interactions are shown. Interacting residues are labeled, and hydrogen bonds are represented with cyan spheres. C) The virtual screening hit compound **1** was predicted to mimic GTP binding (ICM score = −25.5). D) Hit compound **1** was confirmed active in the FtsZ GTPase assay as well as independent antimicrobial susceptibility assays against *E. coli* and *S. aureus*. Other virtual screening hit candidates (Supporting Information Figure S1) were inactive in the assay conditions.

approved antibiotics are either natural products or closely related semisynthetic derivatives inspired by the large scaffold diversity available from natural sources.[29,30] Because several high-resolution X-ray crystal structures of FtsZ are currently available,[10,24,31] structure-based virtual screening is a very attractive approach for the discovery of new FtsZ inhibitors. In this study, the combination of virtual screening and biological evaluation experiments was used to identify a new class of FtsZ inhibitors that might be potentially useful for chemical derivatization into broad-spectrum antibacterial agents.

## MATERIALS AND METHODS

**Protein and Ligand Preparation.** The ICM molecular modeling package version 3.6-1c was used for all computation studies.[32] The FtsZ X-ray crystal structures were retrieved from the RCSB Protein Data Bank (http://www.rcsb.org) and were prepared for the docking simulations using the protein preparation protocol implemented in ICM. Protein preparation is a fully automatic workflow to convert the PDB atom records into MMFF atom types.[33] During this procedure, hydrogens were built, formal charges were assigned, protonation states of histidines were optimized, and glutamine, aspargine, and histidine side chains were flipped to the best hydrogen bonding

network. Co-crystal ligands, water molecules, and ions were removed from the GTP binding site before docking.

A library of approximately 20,000 compounds was downloaded from Analyticon Discovery (http://www.ac-discovery.com) and prepared for virtual screening using the ICM software. Protonation states were calculated at pH 7.4 using an automatic $pK_a$ model, and possible stereoisomers and/or tautomers were generated. After adding hydrogens, MMFF atom types were assigned, and the molecules were converted into 3D and minimized.

**Docking-Based Virtual Screening.** The Analyticon Discovery compounds were docked against the GTP binding site of the 2.2 Å X-ray crystal structure of *M. jannaschii* FtsZ (PDB entry 1W5B) using the ICM software.[10] The GTP binding site was defined as the cavity delimited by residues with at least one non-hydrogen atom within a 4.0 Å cutoff radius from the GTP cocrystal. In order to reduce the time of calculation, binding site residues were considered to be rigid (rigid-protein docking), and the pocket was represented by 0.5 Å grid potential maps accounting for hydrogen bonding, hydrophobic, van der Waals, and electrostatic interactions.[34] The molecules were flexibly docked against the rigid model of the GTP binding site and scored according to the ICM scoring function.[32] Three independent docking runs were performed, and the top-scoring pose of each compound was selected for further analysis.

In order to maximize the chemical diversity for biological screening, binary fingerprints were calculated for each compound, and the molecules were clustered using the unweighted pair group method with arithmetic mean (UPGMA) agglomerative hierarchical algorithm implemented in the ICM software. About one hundred representative top-scoring compounds within clusters with a Tanimoto distance of at least 0.3 were selected for visual inspection. The predicted binding poses were compared with the experimental X-ray cocrystal structure of GTP (Figure 1A). Ten compounds establishing characteristic GTP-like interactions with the enzyme were selected. The molecules were purchased from Analyticon Discovery and tested in the GTPase *in vitro* assay and antimicrobial susceptibility tests. Details on the biological assays are provided on the last sections of the Materials and Methods.

**Induced-Fit Docking.** After the hit compound **1** was confirmed to have a moderate *in vitro* anti-FtsZ activity, induced-fit docking studies were carried out in order to account for the pocket plasticity upon binding of pyrimidine-substituted quinuclidines. The analysis was performed on eight X-ray crystal structures from different bacterial strains (PDB entries 1OFU, 1RLU, 1W5B, 1W5F, 2R6R, 2R75, 2VAP, and 2VXY, Supporting Information Figure S2), using the Scan Alanines and Refine (SCARE) algorithm developed by Bottegoni et al.[35] The SCARE analysis was performed within the ICM molecular modeling environment. Briefly, the algorithm replaced groups of two or three flexible GTP binding site residues by alanines. The list of amino acids selected for alanine mutation is provided in Table 1. The minimum distance between mutating residues was set to 5 Å and 3 Å for dual and triple mutations, respectively. Rigid amino acids such as glycines and prolines were not candidates for alanine mutation. Compound **1** was docked into the alanine-mutated enzyme and a stack of alternative top-scoring poses was saved. After reintroduction of the original mutated residues, the binding poses obtained in the previous step were restrained, and the surrounding side chains were fully optimized using Monte Carlo conformational search. Backbone conformations were kept rigid along the process. Finally, the optimized protein−ligand complexes were rescored, and the top-scoring binding poses of compound **1** against each structure were saved. The top-scoring complex derived from *A. aeolicus* FtsZ (ICM score = −41.2, Table 1) was selected for further analysis.

**Table 1. Induced-Fit Docking of Compound 1 against Multiple Crystal Structures of FtsZ[e]**

| PDB | R (Å)[a] | bacterial strain | alanine mutations[b] | initial score[c] | refined score[d] |
|---|---|---|---|---|---|
| 1OFU | 2.1 | *P. aeruginosa* | Asn25, Arg143, Asp187 | −11.1 | −36.0 |
| 1RLU | 2.1 | *M. tuberculosis* | Asn22, Arg140 | −14.3 | −31.5 |
| 1W5B | 2.2 | *M. jannaschii* | Asn51, Arg169, Asp212 | −25.5 | −32.6 |
| 1W5F | 2.0 | *T. maritima* | Asn35, Arg153, Asp197 | −12.6 | −15.2 |
| 2R6R | 1.7 | *A. aeolicus* | Asn21, Lys139, Asp183 | −22.7 | −41.2 |
| 2R75 | 1.4 | *A. aeolicus* | Asn21, Lys139, Asp183 | −22.6 | −40.1 |
| 2VAP | 1.7 | *M. jannaschii* | Arg169, Asp212 | 5.6 | −25.4 |
| 2VXY | 1.7 | *B. subtilis* | Asn25, Arg143, Asp187 | −4.86 | −22.7 |

[a]Resolution in angstroms. [b]The selected binding site residues were mutated into alanines. [c]ICM binding scores using rigid-protein docking. [d]ICM binding scores after induced-fit docking using the SCARE algorithm. [e]The ICM binding scores prior refinement (initial score), i.e. from rigid-protein docking against the original PDB structures, is also shown for comparison. Lower ICM binding scores indicate stronger protein-ligand interactions.

**Homology Modeling of *S. aureus* FtsZ.** A homology model of *S. aureus* FtsZ was built using the refined *A. aeolicus* structure as template (induced-fit model derived in the previous step, with quinuclidine **1** bound to the GTP site). Sequence alignment was performed using the ZEGA method with gap opening and extension penalties of 2.4 and 0.15, respectively.[36] Subsequently, the homology model was built by inheriting the backbone conformation from the structural template and replacing nonidentical side chains while preventing the change of as many torsion variables as possible.

**Redocking of Pyrimidine-Quinuclidines against the *S. aureus* FtsZ Model.** A library of 675 Analyticon Discovery compounds bearing the pyrimidine-quinuclidine scaffold were redocked against the GTP binding site of the *S. aureus* FtsZ model, using the rigid-protein docking protocol described in the virtual screening section. The top-scoring compounds were visually inspected taking into account the hydrogen bonding network within the GTP binding site, shape, and physicochemical complementarily as well as similarities with the known binding mode of GTP and the predicted induced-fit binding mode of compound **1** (Figure 2). Top-scoring quinuclidines **2**−**10** (Table 2) were purchased and tested in the antimicrobial susceptibility and GTPase inhibition assays.

***In Vitro* Biological Assays.** The purity of all purchased compounds (≥95%) was confirmed by Analyticon Discovery using nuclear magnetic resonance (NMR) or high-performance liquid chromatography (HPLC) and the compounds were used as received. Totarol was purchased from Sigma-Aldrich. Stock solutions were prepared in DMSO. The final percentage of DMSO in the assays was 1% for all experiments. Bacterial

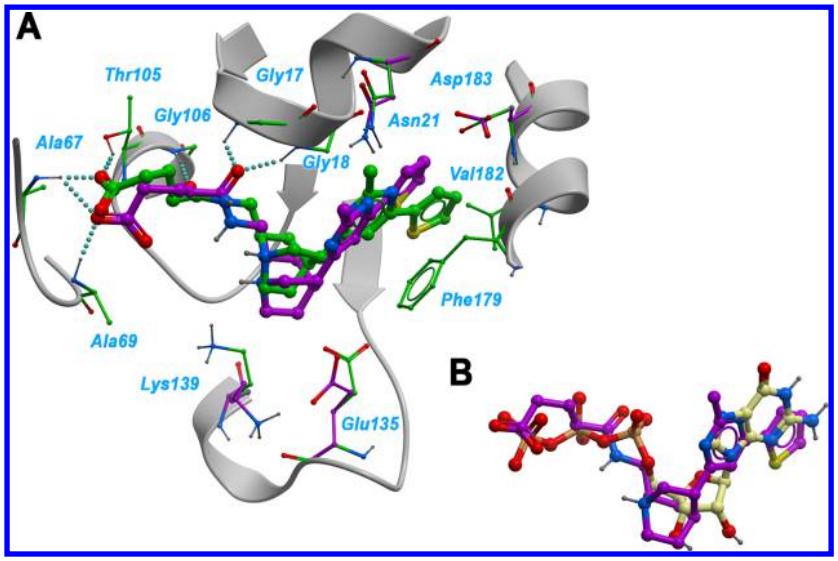


**Figure 2.** The predicted binding mode of compound **1** was refined using fully flexible docking (SCARE algorithm).[35] The GTP binding site residues of *A. aeolicus* FtsZ (PDB entry 2R6R) are labeled and represented with green carbons. Rotated side chains upon fully flexible docking (i.e., Asn21, Glu135, Lys139, and Asp183) are represented with purple carbons. A) Docking poses of compound **1**, predicted using rigid-protein docking (green carbons, ICM score = −22.7) or fully flexible docking (purple carbons, ICM score = −41.2) are shown. The RMSD difference between the two poses was equal to 1.7 Å. B) The fully flexible docking pose of compound **1** mimics the known X-ray cocrystal structure of GTP (yellow carbons) taken from PDB entry 1W5B.

strains were purchased from the American Type Culture Collection (ATCC, USA).

**GTPase Activity Assay.** A detailed description of the *S. aureus* FtsZ cloning and expression is provided as Supporting Information. The GTPase activity of recombinant *S. aureus* FtsZ was measured in a 96-well microplate using a CytoPhos phosphate assay Biochem Kit (Cytoskeleton, USA) according to an optimized protocol based on the manufacturer's instructions. *S. aureus* FtsZ (7.5 $\mu$M) was preincubated with serial dilutions of each compound in 50 mM 4-morpholinepropanesulfonic acid (MOPS, pH 6.5) buffer for 10 min at 25 °C. Control experiments were performed with 1% DMSO instead of the compound solution. Then 5 mM of $MgCl_2$ and 200 mM of KCl were added. Reactions were started with the addition of 500 $\mu$M GTP and incubated at 37 °C. After 30 min, the reactions were quenched by adding 100 $\mu$L of Cytophos reagent. After 10 min incubations, inorganic phosphate was quantified by measuring the absorbance at 650 nm in a microplate reader. Three independent assays were performed in triplicate. The $IC_{50}$ values were determined by nonlinear regression with a sigmoidal concentration−response curve, using the Origin software version 6. Representative concentration−response plots are provided in Supporting Information Figure S3.

**Antimicrobial Susceptibility Assay.** The *in vitro* antimicrobial activity was conducted in 96-well microplates using the broth microdilution procedure in accordance to the Clinical and Laboratory Standards Institute (CLSI) guidelines.[37] Cation-adjusted Mueller Hinton broth for *S. aureus* ATCC 29213 and Mueller Hinton broth for *E. coli* ATCC 25922 were used in the assays. Four to five colonies from overnight cultures of the test bacterial strain on a trypticase soy blood (TSB) agar plate were inoculated in 10 mL of broth for 4−6 h at 37 °C. Then, the inoculum of the bacterial suspension was seeded in a 96-well microplate (final concentration of ~$5 \times 10^5$ CFU/mL) containing 100 $\mu$L of serial dilutions of the tested compounds. Control wells contained either bacterium and medium or medium only. After incubation for 18 h at 37 °C, the absorbance at 600 nm ($A_{600}$) was recorded to calculate the percentage of bacterial cell inhibition with respect to controls, using a microplate reader. Three independent assays were performed for each test.

**Tubulin Polymerization Assay.** The effects of quinuclidine **12** on bovine brain tubulin polymerization were tested using the Tubulin Polymerization Assay Kit (Cytoskeleton, USA) according to the manufacturer's instructions. Bovine brain tubulin was used at a final concentration of 2 $\mu$g/mL. Quinuclidine **12** (500 $\mu$M) was tested in a concentration more than ten times its $IC_{50}$ value for *S. aureus* FtsZ. Paclitaxel (20 $\mu$M) and vinblastine (3 $\mu$M) were also included as reference compounds. The final DMSO concentration in the assays and control was always 1%. Fluorescence was measured using a PolarStar Optima (BMG Labtech, Offenburg, Germany) microplate reader at excitation and emission wavelengths of 360 and 450 nm, respectively. Data were collected using a Microsoft Excel spreadsheet and treated using the Origin 6.0 software. Three independent assays were performed in triplicate.

## RESULTS AND DISCUSSION

**Structure-Based Virtual Screening and Biological Evaluation of New FtsZ Inhibitors.** Discovery of novel antibacterials via targeting the GTP binding site of FtsZ may have an advantage over other domains such as the T7 loop and the H7 helix. Several FtsZ inhibitors, such as cinnamaldehyde and PC190723, were found to bind to the T7 loop or the H7 helix at the C-terminus domain.[20,23] However, they only inhibited Gram-positive bacterial strains. One possible reason is that they bind to a less conserved domain. Indeed, the C-terminal domain of FtsZ is the most variable region among Gram-positive and Gram-negative bacterial strains.[5] On the opposite, the GTP binding site at the N-terminal is highly conserved. Thus, targeting the GTP binding site might offer a better chance of developing broad-spectrum antibacterial

Table 2. FtsZ GTPase Inhibition and Antimicrobial Activity of Pyrimidine Substituted Quinuclidines 1−20 and Totarol

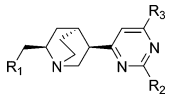

| Cmpd | $R_1$ | $R_2$ | $R_3$ | $IC_{50}$ (μM)[a] | MIC (μM)[b] *S. aureus* | MIC (μM)[b] *E. coli* |
|---|---|---|---|---|---|---|
| 1 | 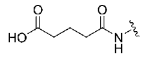 | $CH_3$ |  | 317.2 ± 17.0 | 897.1 | 449.0 |
| 2 | 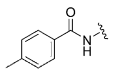 | $CH_3$ |  | >1000 | 444.4 | 222.2 |
| 3 | 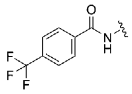 | $CH_3$ |  | 696.9 ± 12.3 | 49.4 | 74.1 |
| 4 |  | $CH_3$ |  | 399.3 ± 12.0 | 248.7 | 248.7 |
| 5 |  | $CH_3$ |  | >1000 | >1000 | >1000 |
| 6 | 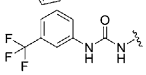 | $CH_3$ |  | 544.5 ± 87.8 | 47.8 | 127.6 |
| 7 |  | $CH_3$ |  | 190.3 ± 12.6 | 91.3 | 162.2 |
| 8 |  | $CH_3$ |  | >1000 | >1000 | >1000 |
| 9 | 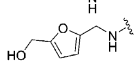 | $CH_3$ |  | >1000 | >1000 | >1000 |
| 10 | 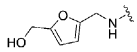 |  |  | 73.2 ± 4.1 | 50.5 | 75.7 |
| 11 |  |  |  | 55.7 ± 2.4 | 26.9 | 161.6 |
| 12 |  |  |  | 37.5 ± 2.2 | 24.6 | 49.2 |
| 13 |  |  |  | 188.7 ± 9.1 | 126.4 | 126.4 |
| 14 |  |  |  | >500 | >200 | >200 |
| 15 |  |  |  | >500 | >200 | >200 |
| 16 | 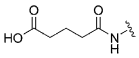 |  |  | >500 | >200 | >200 |
| 17 |  |  |  | >500 | >200 | >200 |
| 18 |  |  |  | >500 | >200 | >200 |
| 19 |  |  |  | >500 | >200 | >200 |
| 20 |  |  |  | >500 | >200 | >200 |
| Totarol | | | | 40.8 ± 15.1 | 5.3 | >1397 |

[a]FtsZ GTPase inhibition $IC_{50}$ ± SEM ($n$ = 3). [b]*S. aureus* and *E. coli* MIC values.

agents. A few FtsZ inhibitors have already been reported to bind into the GTP binding site, such as berberine and chrysophaentin A.[22,38]

The crystal structure of *M. jannaschii* FtsZ (PDB entry 1W5B)[10] was used to perform virtual ligand screening of natural products and semisynthetic derivatives available from


dx.doi.org/10.1021/ci400203f | J. Chem. Inf. Model. 2013, 53, 2131−2140

Analyticon Discovery. Out of approximately 20,000 molecules screened in this study, about 2,400 compounds were natural products isolated from plants and microorganisms, that have been previously shown to provide a good scaffold diversity for drug discovery projects.[39] Moreover, the screening database was further enriched with semisynthetic derivatives available from the same vendor, in order to increase the R-group diversity and derive the preliminary structure−activity relationships.

Because natural antibacterial agents do not generally follow the Lipinski Rule of five criteria for absorption and permeation, no physicochemical property filtering was used prior to docking.[40] ICM was used to globally optimize the internal coordinates of each molecule in the space of grid potential maps calculated for the GTP binding site, and an estimate of the protein−ligand binding affinity was calculated for each compound using the ICM scoring function.[32,41] The scoring takes into account van der Waals interactions, electrostatic potential, hydrogen bonding, entropy, and desolvation energy differences between bound and unbound states of the ligand.[42] Chemically diverse top-scoring binding modes were then visually inspected using the known cocrystal structure of the GTP substrate as a reference. As shown in Figure 1A, the GTP binding site is largely exposed to the solvent and predominantly polar. The GTP substrate binds through an extensive network of hydrogen bonds between the triphosphate and the backbone amide groups of Gly47, Ala48, Ala97, Gly99, Gly134, Thr135, and Gly136 (Figure 1B). The GTP ribose establishes hydrogen bonds with Arg169 and Glu165, and the guanine accommodates into a binding cleft delimited by Ala48, Asn51, Phe208, and Asp212. van der Walls interactions as well as a pair of hydrogen bonds with Asp212 are important for further stabilization of the FtsZ-GTP complex.

Ten compounds predicted to establish GTP-like contacts with the enzyme were selected for biochemical evaluation (compound **1** in Figure 1D and compounds **S1**−**S9** in Supporting Information Figure S1). The molecules, selected among the top-scoring virtual screening hit compounds, were predicted to establish a similar pattern of hydrogen bonds, providing a good overlap with the native GTP cocrystal structure. Moreover, the compounds were predicted to establish similar hydrophobic interactions within the guanidine cleft. These molecules were purchased and tested *in vitro*.

In order to assess the potential inhibitory activity against the bacterial cell division protein FtsZ, the compounds were tested in the standard GTPase activity assay. The GTPase inhibitory activity was determined by measuring the concentration at which the compounds inhibited 50% of the GTP hydrolysis. Moreover, the molecules were also tested in the antimicrobial susceptibility assay against two clinically relevant bacterial strains, i.e. Gram-negative *E. coli* ATCC 25922 and Gram-positive *S. aureus* ATCC 29213. The minimum inhibitory concentration (MIC) was defined as the lowest concentration of the tested compound that inhibited ≥90% bacterial growth when compared to the control. The results of these two independent assays confirmed that compound **1**, i.e. 4-(((2*R*,4*S*,5*R*)-5-(2-methyl-6-(thiophen-2-yl)pyrimidin-4-yl)-quinuclidin-2-yl)methylcarbamoyl)butanoic acid (Figure 1C), inhibited the FtsZ GTPase activity with typical sigmoidal concentration−response curve ($IC_{50}$ = 317.2 μM) and was active against both bacterial strains (*E. coli* and *S. aureus* MIC values of 449.0 μM and 897.1 μM, respectively). The remaining virtual screening hit compounds **S1**−**S9** (Supporting Information Figure S1) were inactive in both assays at concentrations up to 384 μg/mL.

Despite its moderate anti-FtsZ potency, compound **1** was active against both Gram-positive and Gram-negative bacteria and has a new molecular scaffold (pyrimidine-quinuclidine) not previously studied for antibacterial purposes. Based on the screening results, compound **1** was selected as a starting hit for further *in silico* optimization and structure−activity relationships analysis.

**Induced-Fit Docking of Compound 1 into the GTP Binding Site of FtsZ.** Rigid-protein docking is one of the most common approaches to perform virtual screening of large compound databases. Two main advantages are the shorter times required for the processing of large electronic databases and the lower false positive rates than fully flexible docking.[43] However, rigid-protein docking neglects conformational plasticity upon binding of compounds from different chemotypes, a common phenomenon that is often important for proper steric fit and physiochemical complementarity within the protein pocket.

Superimposition of the GTP binding sites of FtsZ from different bacterial strains revealed a highly rigid backbone with less than 0.8 Å pairwise RMSD differences (Supporting Information Figure S2). Despite the backbone rigidity, the side chains of some active site amino acids such as Asn51, Arg169, and Asp212 are highly flexible. In order to account for the potential induced-fit movements of the GTP binding site bound to pyrimidine-quinuclidine derivatives, we used the induced-fit docking algorithm Scan Alanines and Refine (SCARE)[35] to optimize the predicted binding mode of compound **1**. The SCARE algorithm explores the conformational flexibility of amino acid side chains, while keeping the protein backbone rigid, and is a fast and effective approach to explore the side-chain plasticity of relatively rigid pockets. In order to incorporate additional experimentally known fluctuations of the GTP binding site, the analysis was extended to a set of eight alternative X-ray crystal structures of FtsZ available from the PDB database. Other approaches commonly used to simulate the backbone movements include, for example, molecular dynamics simulations and elastic network normal-mode analysis.[43]

Fully flexible docking with the SCARE algorithm predicted energetically more favorable protein−ligand complexes than the rigid-protein docking (Table 1). Binding mode predictions, before and after the induced-fit docking, were essentially similar; however, slight readjustments at the GTP binding site led to a larger number of favorable protein−ligand contacts. The top-scoring pose upon refinement with the SCARE algorithm was observed with the crystal structure of the *A. aeolicus* FtsZ (PDB entry 2R6R, refined score = −41.2).[31] As shown in Figure 2A, burial of compound **1** into the GTP binding site increased after slight readjustments of the side chains of Asn21, Glu135, Lys139, and Asp183, corresponding to 1W5B residues Asn51, Glu165, Arg169, and Asp212. Repositioning of the Glu135 was of particular importance for the readjustment, as the rotation along the Cβ−Cγ axis created the extra space for fitting the bulky quinuclidine moiety into the GTP site and reoriented the negatively charged carboxylic acid toward the solvent, therefore, exposing hydrophobic atoms of the Glu135 side chain toward the apolar quinuclidine core. These findings suggest that the predicted induced-fit movements for binding of pyrimidine-substituted quinuclidines might be important for docking of new derivative compounds.

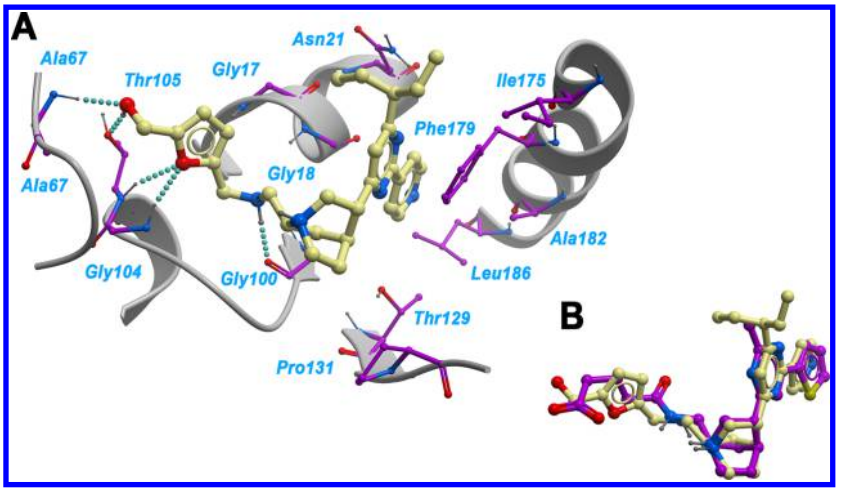


**Figure 3.** Predicted binding mode of pyrimidine-substituted quinuclidine **10** (yellow carbons) into the GTP binding site of *S. aureus* FtsZ. A) Interacting residues are labeled and shown in 'ball and sticks'. Hydrogen bonds are indicated by cyan spheres. B) The predicted docking pose of quinuclidine **1** (purple carbons) is shown for comparison.

Quinuclidine **1** mimics native interactions of the endogenous GTP substrate with the enzyme. As shown in Figure 2A, the 4-carbamoylbutanoic acid fits into the triphosphate binding pocket and establishes hydrogen bonds with Gly17, Gly18, Ala67, and Ala69. The quinuclidine mimics the sugar moiety as a rigid linker. Similar to the GTP purine, $\pi$-stacking interactions between the pyrimidine ring of compound **1** and the phenyl moiety of Phe179 were found (Figure 2A). The pyrimidine-bound thiophene extends into a small hydrophobic subpocket adjacent to the purine binding site delimited by Val182 and Leu186.

**Homology Modeling of *S. aureus* FtsZ.** Despite the high 3D structure conservation among FtsZ enzymes from different bacterial strains, a model of *S. aureus* FtsZ might be important for a better understanding of the structure–activity relationships derived from the GTPase assay with recombinant *S. aureus* protein. By the time this study was performed, the X-ray crystal structure of *S. aureus* FtsZ was not available. Therefore, the top-scoring induced-fit model derived from *A. aeolicus* FtsZ (PDB entry 2R6R) was used as a structural template to build a homology model. Quinuclidine **1** was left inside the GTP binding site along the homology modeling steps, in order to preserve the shape of the pocket, as well as the most important protein–ligand contacts refined with SCARE. *S. aureus* FtsZ shares high sequence identity with the *A. aeolicus* counterpart, and, therefore, the amino acid sequence alignment was straightforward. Five *A. aeolicus* FtsZ GTP binding site residues (Lys70, Leu101, Leu130, Lys139, and Val182) were mutated into the corresponding residues of the *S. aureus* FtsZ (Asn74, Met105, Arg134, Arg143, and Ala186, respectively). Of these, only Val182 and Lys139 were directly pointing toward the inside of the GTP binding site (Figure 2). The valine to alanine mutation generated extra space into the GTP binding site that might have an impact for binding of bulky pyrimidine substituents. Finally, the GTP binding site of *S. aureus* FtsZ, with quinuclidine **1** bound under position restraints, was refined using Monte Carlo conformational search.

Redocking of compound **1** against the *S. aureus* FtsZ model provided nearly the same binding mode, as compared to *A. aeolicus* FtsZ, yet slightly higher binding score (RMSD = 0.9 Å, ICM score = −37.5). Therefore, the *S. aureus* FtsZ model was selected for the screening of new quinuclidine derivatives and SAR analysis.

**Structure–Activity Relationships Derived from Quinuclidine-Based FtsZ Inhibitors.** During the initial virtual screening against PDB entry 1W5B, most of the quinuclidine derivatives had relatively low ICM scores. Some exceptions include quinuclidine **1** and close analogs able to establish a similar pattern of hydrogen bonds within the triphosphate binding pocket. Quinuclidine **1**, the top-scoring molecule among this series, was thus selected for biological evaluation.

In order to assess some preliminary structure–activity relationships of FtsZ inhibitors bearing the pyrimidine-quinuclidine scaffold, commercially available compound **1** analogs were redocked against the *S. aureus* FtsZ model. As expected, the refined ICM docking scores were significantly better than those obtained during the initial virtual screening. Quinuclidines **2**–**10** (Table 2) were selected among the top-scoring compounds and purchased for the *in vitro* assays. These molecules were predicted to establish a pattern of interactions within the GTP binding site similar to compound **1**. Totarol, a commercially available FtsZ inhibitor, was also tested in the same conditions and used as a reference compound.

Most of the compounds in a series of 2-methyl-6-(thiophen-2-yl)pyrimidin-4-yl-quinuclidines (compounds **2**–**7**, Table 2) had stronger antimicrobial potency than the initial hit **1**, with the lowest MIC values being found with **3** (*S. aureus* MIC = 49.4 $\mu$M, *E. coli* MIC = 74.1 $\mu$M) and **6** (*S. aureus* MIC = 47.8 $\mu$M, *E. coli* MIC = 127.6 $\mu$M). Interestingly, both molecules share a trifluoromethyl group that is well-known to increase lipophilicity and favor bacterial cell permeation.[44] Lack of the negatively charged carboxylic acid ($R_1$-substituent) might also have contributed for an increased bacterial permeation. However, despite these significant improvements in the antimicrobial activity, compounds **3** and **6** were less potent against the FtsZ GTPase activity than compound **1**. Also within this series, quinuclidine **7** equipped with a N-(2-methylfuran) at the $R_1$-position showed good potency improvements in both assays ($IC_{50}$ = 190.3 $\mu$M, *S. aureus* MIC = 91.3 $\mu$M, *E. coli* MIC = 162.2 $\mu$M).

Antibacterial activity improvements of 6- and 18-fold were achieved with quinuclidine **10**, as compared to the initial hit **1**, against *E. coli* (MIC = 75.7 $\mu$M) and *S. aureus* (MIC = 50.5


dx.doi.org/10.1021/ci400203f | J. Chem. Inf. Model. 2013, 53, 2131–2140

$\mu$M), respectively. The FtsZ GTPase inhibition potency was also increased by a factor of 4 ($IC_{50}$ = 73.2 $\mu$M, Table 2). Compound **10** is equipped with furfuryl alcohol bound to the quinuclidine moiety, and pyridine/pentanyl substituents bound to the pyrimidine ring, instead of the carbamoylbutanoic acid, methyl, and thiophene in compound **1**. As shown in Figure 3A, the noncharged furfuryl alcohol in compound **10** preserved a similar pattern of hydrogen bonds within the triphosphate binding site while reducing the overall net charge of the molecule. The pyrimidine moiety of compound **10** was predicted to rotate by 180 degrees, as compared to compound **1**, projecting the pyridine ring ($R_2$-substituent) toward the guanine binding site. At the top of the GTP binding groove, the 3-pentanyl interacts with hydrophobic residues such as Phe179 and Ile175. These encouraging results prompted us to further explore the structure−activity relationships of 6-(pentan-3-yl)-2-(pyridine-4-yl)pyrimidin-4-yl-quinuclidines with a new set of commercially available quinuclidines. Ten compounds, selected with a substructure search (**11**−**20**, Table 2), were purchased from Analyticon Discovery and tested *in vitro*. It is worth noting that although not all of these molecules were among the top-scoring compounds, e.g. compounds **11**, **12**, and **13** had −19.1, −16.2, and −12.2 ICM scores, they were interesting from a medicinal chemistry point of view to explore the structure−activity relationships of the $R_1$-substituent.

Compound **11** bearing the N-(2-methylfuran) $R_1$-substituent showed slight potency improvements against the Gram-positive *S. aureus* (MIC = 26.9 $\mu$M) as well as against the GTPase activity of recombinant *S. aureus* FtsZ ($IC_{50}$ = 55.7 $\mu$M), but the activity was deteriorated against Gram-negative *E. coli* (MIC = 161.6 $\mu$M) as compared to the parent compound **10**. Interestingly, the most potent quinuclidine derivative identified in this study was obtained by further 'trimming' of the $R_1$-substituent into a primary amine (**12**), suggesting that the triphosphate binding site interaction is not essential for the FtsZ inhibition. The antibacterial activities against *S. aureus* (MIC = 24.6 $\mu$M) and *E. coli* (MIC = 49.2 $\mu$M) improved up to 2-folds, as compared to those of compound **10**, and a similar potency improvement against the GTPase activity was found ($IC_{50}$ = 37.5 $\mu$M).

Our biological evaluation of the natural FtsZ inhibitor totarol was in good agreement with recent publications reporting high potency against Gram-positive bacteria but no activity against Gram-negative strains.[21] Several mechanisms of antibacterial action against Gram-positive bacteria have been reported, including not only the inhibition of the GTPase activity of FtsZ but also inhibition of multidrug efflux pumps,[45] inhibition of the bacterial electron transport chain,[46] and perturbation of the physical properties of the Gram-positive bacterial membrane.[47] Quinuclidine **12** was slightly more potent than totarol against the GTPase activity of FtsZ ($IC_{50}$ = 40.8 $\mu$M, Table 2) suggesting equipotent protein−ligand interactions. In addition, compound **12** showed stronger antibacterial activity than totarol against the Gram-negative strain of *E. coli*, which may indicate a broader spectrum of antibacterial activity. The stronger potency of totarol against *S. aureus* might be related to the other mechanisms of antibacterial activity. In summary, the chemical optimization of virtual screening hit compound **1** into lower molecular weight FtsZ inhibitors suggests that the pyrimidine-quinuclidine scaffold is an interesting new chemotype for the development of broad-spectrum antibacterial agents. Indeed, compound **12** not only improved the antibacterial activity but also is significantly smaller than its parent compound **1** and has more favorable lead-like properties such as less hydrogen bonding groups and rotatable bonds and lower molecular volume and polar surface area.

The potent GTPase activity of quinuclidine **12** devoid of the typical hydrogen bond interactions within the triphosphate binding site suggests that the virtual screening strategy could be recalibrated and extended to a larger set of compounds. Solvent exposed binding pockets such as the GTP binding site of FtsZ are well-known to deteriorate the docking and scoring performance.[48] Reducing the weight of the hydrogen bonding contribution for protein−ligand interactions at the solvent-exposed surface could be an effective approach to decrease the false positive rates. Moreover, because protein−ligand contacts within the triphosphate binding site are not critically important for inhibition of the GTPase activity, site-specific weights could be created to reward protein−ligand contacts within the sugar and nucleotide binding regions, rather than within the triphosphate site.

**Effects on Mammalian Tubulin Polymerization.** Targeting the highly conserved GTP binding site of FtsZ is an appealing approach for development of broad-spectrum antibacterial agents. However, because GTP binding sites are common to a number of human proteins, FtsZ inhibitors might have potential liabilities related to the off-target-associated activity. Among the potential off-targets of FtsZ inhibitors, the mammalian tubulin is of upmost importance. Despite its weak sequence homology to bacterial FtsZ, mammalian tubulin shares similar structural and functional properties and therefore should be carefully evaluated as a potential off-target of FtsZ inhibitors.

The effects of compound **12** on bovine brain tubulin polymerization were monitored by fluorescence microscopy after incorporation of a fluorescent reporter (DAPI) into the microtubules. A known tubulin polymerization enhancer (paclitaxel) and a known inhibitor of tubulin-dependent GTP hydrolysis (vinblastine) were tested as reference compounds in the same assay conditions.[49] As shown in Figure 4, the fluorescence intensity was significantly increased in the presence of paclitaxel (20 $\mu$M), confirming that the rate of polymerization was significantly enhanced. On the opposite, vinblastine (30 $\mu$M) completely inhibited the polymerization of mammalian tubulin. Quinuclidine **12** (500 $\mu$M) provided

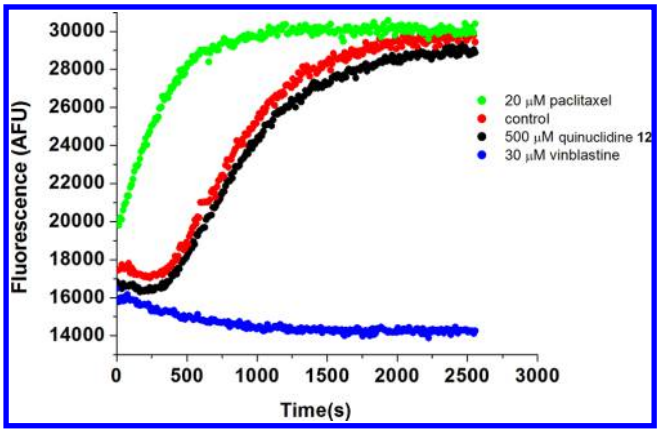


**Figure 4.** Polymerization of mammalian tubulin in the absence (red) and in the present of 500 $\mu$M of compound **12** (black). Twenty $\mu$M Paclitaxel (green) and 30 $\mu$M vinblastine (blue) were also used for comparison. The results represent the average of three independent experiments ($n$ = 3).


dx.doi.org/10.1021/ci400203f | J. Chem. Inf. Model. 2013, 53, 2131−2140

similar results to a control experiment with untreated mammalian tubulin, confirming that compound **12** did not affect tubulin polymerization. In summary, our results suggest that quinuclidine **12** is selective against FtsZ rather than the eukaryotic cytoskeletal tubulin protein.

## CONCLUSION

The combination of structure-based virtual screening, substructure searches, and *in vitro* assays was an effective approach to identify pyrimidine-substituted quinuclidines as a novel chemotype for FtsZ inhibitors. Virtual screening was important for the initial hit identification, while analogue searches and docking were used for the hit optimization steps. Quinuclidine **12** is a small molecular weight compound with low micromolar $IC_{50}$ on the FtsZ GTPase assay and broad-spectrum antibacterial activity against Gram-positive and Gram-negative bacteria. Moreover, this compound strongly inhibited the FtsZ assembly without affecting the polymerization of mammalian tubulin.

Induced-fit docking with the SCARE algorithm provided insights into the molecular basis of binding. The quinuclidine inhibitors were predicted to mimic the endogenous GTP substrate and establish key interactions within the triphosphate, sugar, and nucleotide binding regions. However, the SAR analysis suggested that the polar interactions within the triphosphate binding site are not essential for activity. Although the predicted binding modes are consistent with the GTPase inhibition activity of the compounds found in this study, additional biological studies should be performed in order to confirm the interaction with the GTP binding site of FtsZ, such as protein cocrystallization experiments or competition Saturation Transfer Difference (STD) NMR assays using nonhydrolyzable GTP analogue, guanosine 5′-O-(3-thiotriphosphate) (GTPγS), a high-affinity substrate analogue.[50,51]

The natural compounds from Analyticon Discovery provided a large pool of chemically diverse scaffolds for this study.[39] Although the quinuclidine core has already proved useful for the development of antimalarial, antiparasitic, and antipsychotic agents,[52−54] this is the first report on FtsZ inhibition and antibacterial activity. Given the novel molecular scaffold and the encouraging *in vitro* results, pyrimidine-substituted quinuclidines are a promising new chemotype for further chemical optimization into potent and selective FtsZ inhibitors.

## ASSOCIATED CONTENT

### Supporting Information

Supporting Figure S1 with the virtual screening hit compounds **S1**−**S9**, Supporting Figure S2 with a structural alignment of eight FtsZ GTP binding sites, and Supporting Figure S3 with the concentration−response curves of compounds **1**, **10**, and **12** in the GTPase assay. Description of the *S. aureus* FtsZ cloning and expression. This material is available free of charge via the Internet at http://pubs.acs.org.

## AUTHOR INFORMATION

### Corresponding Author

*Phone: (+852) 34003977. Fax: (+852) 23649932. E-mail: bckywong@polyu.edu.hk.

### Notes

The authors declare no competing financial interest.

## ACKNOWLEDGMENTS

This work was supported by the Research Grants Council (PolyU 5030/11P), the Innovation Technology Commission, and The Hong Kong Polytechnic University.

## REFERENCES

(1) Levy, S. B.; Marshall, B. Antibacterial resistance worldwide: causes, challenges and responses. *Nat. Med.* **2004**, *10*, S122−S129.
(2) Rasko, D. A.; Sperandio, V. Anti-virulence strategies to combat bacteria-mediated disease. *Nat. Rev. Drug Discovery* **2010**, *9*, 117−128.
(3) Klevens, R. M.; Morrison, M. A.; Nadle, J.; Petit, S.; Gershman, K.; Ray, S.; Harrison, L. H.; Lynfield, R.; Dumyati, G.; Townes, J. M.; Craig, A. S.; Zell, E. R.; Fosheim, G. E.; McDougal, L. K.; Carey, R. B.; Fridkin, S. K. Invasive methicillin-resistant *Staphylococcus aureus* infections in the United States. *J. Am. Med. Assoc.* **2007**, *298*, 1763−1771.
(4) Acar, J. F. Consequences of bacterial resistance to antibiotics in medical practice. *Clin. Infect. Dis.* **1997**, *24*, S17−S18.
(5) Erickson, H. P. FtsZ, a prokaryotic homolog of tubulin. *Cell* **1995**, *80*, 367−370.
(6) Addinall, S. G.; Holland, B. The tubulin ancester, FtsZ, draughtsman, designer and driving force for bacterial cytokinesis. *J. Mol. Biol.* **2002**, *318*, 219−236.
(7) Erickson, H. P. FtsZ, a tubulin homologue in prokaryote cell division. *Trends Cell Biol.* **1997**, *7*, 362−367.
(8) Margolin, W. Themes and variations in prokaryotic cell division. *FEMS Microbiol. Rev.* **2000**, *24*, 531−548.
(9) Bi, E.; Lutkenhaus, J. FtsZ ring structure associated with division in *Escherichia coli*. *Nature* **1991**, *354*, 161−164.
(10) Oliva, M. A.; Cordell, S. C.; Lowe, J. Structural insights into FtsZ protofilament formation. *Nat. Struct. Mol. Biol.* **2004**, *11*, 1243−1250.
(11) Adams, D. W.; Errington, J. Bacterial cell division: assembly, maintenance and disassembly of the Z ring. *Nat. Rev. Microbiol.* **2009**, *7*, 642−653.
(12) Margolin, W. FtsZ and the division of prokaryotic cells and organelles. *Nat. Rev. Mol. Cell Biol.* **2005**, *6*, 862−871.
(13) Payne, D. J.; Gwynn, M. N.; Holmes, D. J.; Pompliano, D. L. Drugs for bad bugs: confronting the challenges of antibacterial discovery. *Nat. Rev. Drug Discovery* **2007**, *6*, 29−40.
(14) Lock, R. L.; Harry, E. J. Cell-division inhibitors: new insights for future antibiotics. *Nat. Rev. Drug Discovery* **2008**, *7*, 324−338.
(15) Li, Z. R.; Garner, A. L.; Gloeckner, C.; Janda, K. D.; Carlow, C. K. Targeting the *Wolbachia* cell division protein FtsZ as a new approach for antifilarial therapy. *PLoS Neglected Trop. Dis.* **2011**, *5*, e1411.
(16) Margalit, D. N.; Romberg, L.; Mets, R. B.; Hebert, A. M.; Mitchison, T. J.; Kirschner, M. W.; RayChaudhuri, D. Targeting cell division: small-molecule inhibitors of FtsZ GTPase perturb cytokinetic ring assembly and induce bacterial lethality. *Proc. Natl. Acad. Sci. U. S. A.* **2004**, *101*, 11821−11826.
(17) Urgaonkar, S.; La Pierre, H. S.; Meir, I.; Lund, H.; RayChaudhuri, D.; Shaw, J. T. Synthesis of antimicrobial natural products targeting FtsZ: (±)-dichamanetin and (±)-2‴hydroxy-5″-benzylisouvarinol-B. *Org. Lett.* **2005**, *7*, 5609−5612.
(18) Beuria, T. K.; Santra, M. K.; Panda, D. Sanguinarine blocks cytokinesis in bacteria by inhibiting FtsZ assembly and bundling. *Biochemistry* **2005**, *44*, 16584−16593.
(19) Stokes, N. R.; Sievers, J.; Barker, S.; Bennett, J. M.; Brown, D. R.; Collins, I.; Errington, V. M.; Foulger, D.; Hall, M.; Halsey, R.; Johnson, H.; Rose, V.; Thomaides, H. B.; Haydon, D. J.; Czaplewski, L. G.; Errington, J. Novel inhibitors of bacterial cytokinesis identified by a cell-based antibiotic screening assay. *J. Biol. Chem.* **2005**, *280*, 39709−39715.
(20) Domadia, P.; Swarup, S.; Bhunia, A.; Sivaraman, J.; Dasgupta, D. Inhibition of bacterial cell division protein FtsZ by cinnamaldehyde. *Biochem. Pharmacol.* **2007**, *74*, 831−840.

(21) Jaiswal, R.; Beuria, T. K.; Mohan, R.; Mahajan, S. K.; Panda, D. Totarol inhibits bacterial cytokinesis by perturbing the assembly dynamics of FtsZ. *Biochemistry* **2007**, *46*, 4211−4220.
(22) Plaza, A.; Keffer, J. L.; Bifulco, G.; Lloyd, J. R.; Bewley, C. A. Chrysophaentins A-H, antibacterial bisdiarylbutene macrocycles that inhibit the bacterial cell division protein FtsZ. *J. Am. Chem. Soc.* **2010**, *132*, 9069−9077.
(23) Haydon, D. J.; Stokes, N. R.; Ure, R.; Galbraith, G.; Bennett, J. M.; Brown, D. R.; Baker, P. J.; Barynin, V. V.; Rice, D. W.; Sedelnikova, S. E.; Heal, J. R.; Sheridan, J. M.; Aiwale, S. T.; Chauhan, P. K.; Srivastava, A.; Taneja, A.; Collins, I.; Errington, J.; Czaplewski, L. G. An inhibitor of FtsZ with potent and selective anti-staphylococcal activity. *Science* **2008**, *321*, 1673−1675.
(24) Tan, C. M.; Therien, A. G.; Lu, J.; Lee, S. H.; Caron, A.; Gill, C. J.; Lebeau-Jacob, C.; Benton-Perdomo, L.; Monteiro, J. M.; Pereira, P. M.; Elsen, N. L.; Wu, J.; Deschamps, K.; Petcu, M.; Wong, S.; Daigneault, E.; Kramer, S.; Liang, L.; Maxwell, E.; Claveau, D.; Vaillancourt, J.; Skorey, K.; Tam, J.; Wang, H.; Meredith, T. C.; Sillaots, S.; Wang-Jarantow, L.; Ramtohul, Y.; Langlois, E.; Landry, F.; Reid, J. C.; Parthasarathy, G.; Sharma, S.; Baryshnikova, A.; Lumb, K. J.; Pinho, M. G.; Soisson, S. M.; Roemer, T. Restoring methicillin-resistant *Staphylococcus aureus* susceptibility to $\beta$-lactam antibiotics. *Sci. Transl. Med.* **2012**, *4*, 126ra35.
(25) Jorgensen, W. L. The many roles of computation in drug discovery. *Science* **2004**, *303*, 1813−1818.
(26) Bajorath, F. Integration of virtual and high-throughput screening. *Nat. Rev. Drug Discovery* **2002**, *1*, 882−894.
(27) Simmons, K. J.; Chopra, I.; Fishwick, C. W. G. Structure-based discovery of antibacterial drugs. *Nat. Rev. Microbiol.* **2010**, *8*, 501−510.
(28) Rollinger, J. M.; Stuppner, H.; Langer, T. Virtual screening for the discovery of bioactive natural products. In *Natural Compounds as Drugs, Vol 1*; Petersen, F., Amstutz, R., Eds.; **2008**; Vol. *65*, pp 211−249.
(29) Newman, D. J.; Cragg, G. M. Natural products as sources of new drugs over the last 25 years. *J. Nat. Prod.* **2007**, *70*, 461−477.
(30) Harvey, A. L. Natural products in drug discovery. *Drug Discovery Today* **2008**, *13*, 894−901.
(31) Oliva, M. A.; Trambaiolo, D.; Loewe, J. Structural insights into the conformational variability of FtsZ. *J. Mol. Biol.* **2007**, *373*, 1229−1242.
(32) Neves, M. A. C.; Totrov, M.; Abagyan, R. Docking and scoring with ICM: the benchmarking results and strategies for improvement. *J. Comput.-Aided Mol. Des.* **2012**, *26*, 675−686.
(33) Halgren, T. A. Merck molecular force field. I. Basis, form, scope, parameterization, and performance of MMFF94. *J. Comput. Chem.* **1996**, *17*, 490−519.
(34) An, J. H.; Totrov, M.; Abagyan, R. Pocketome via comprehensive identification and classification of ligand binding envelopes. *Mol. Cell. Proteomics* **2005**, *4*, 752−761.
(35) Bottegoni, G.; Kufareva, I.; Totrov, M.; Abagyan, R. A new method for ligand docking to flexible receptors by dual alanine scanning and refinement (SCARE). *J. Comput.-Aided Mol. Des.* **2008**, *22*, 311−325.
(36) Abagyan, R. A.; Batalov, S. Do aligned sequences share the same fold? *J. Mol. Biol.* **1997**, *273*, 355−368.
(37) Clinical and Laboratory Standards Institute (CLSI), methods for dilution antimicrobial susceptibility tests for bacteria that grow aerobically; approved standard seventh edition.
(38) Domadia, P. N.; Bhunia, A.; Sivaraman, J.; Swarup, S.; Dasgupta, D. Berberine targets assembly of *Escherichia coli* cell division protein FtsZ. *Biochemistry* **2008**, *47*, 3225−3234.
(39) Yongye, A. B.; Waddell, J.; Medina-Franco, J. L. Molecular scaffold analysis of natural products databases in the public domain. *Chem. Biol. Drug Des.* **2012**, *80*, 717−724.
(40) Ganesan, A. The impact of natural products upon modern drug discovery. *Curr. Opin. Chem. Biol.* **2008**, *12*, 306−317.
(41) Abagyan, R.; Totrov, M. Biased probability Monte Carlo conformational searches and electrostatic calculations for peptides and proteins. *J. Mol. Biol.* **1994**, *235*, 983−1002.
(42) Schapira, M.; Abagyan, R.; Totrov, M. Nuclear hormone receptor targeted virtual screening. *J. Med. Chem.* **2003**, *46*, 3045−3059.
(43) Rueda, M.; Totrov, M.; Abagyan, R. ALiBERO: evolving a team of complementary pocket conformations rather than a single leader. *J. Chem. Inf. Model.* **2012**, *52*, 2705−2714.
(44) Bohm, H. J.; Banner, D.; Bendels, S.; Kansy, M.; Kuhn, B.; Muller, K.; Obst-Sander, U.; Stahl, M. Fluorine in medicinal chemistry. *ChemBioChem* **2004**, *5*, 637−643.
(45) Smith, E. C.; Kaatz, G. W.; Seo, S. M.; Wareham, N.; Williamson, E. M.; Gibbons, S. The phenolic diterpene totarol inhibits multidrug efflux pump activity in *Staphylococcus aureus*. *Antimicrob. Agents Chemother.* **2007**, *51*, 4480−4483.
(46) Haraguchi, H.; Oike, S.; Muroi, H.; Kubo, I. Mode of antibacterial action of totarol, a diterpene from *Podocarpus nagi*. *Planta Med.* **1996**, *62*, 122−125.
(47) Foss, M. H.; Eun, Y. J.; Grove, C. I.; Pauw, D. A.; Sorto, N. A.; Rensvold, J. W.; Pagliarini, D. J.; Shaw, J. T.; Weibel, D. B. Inhibitors of bacterial tubulin target bacterial membranes. *MedChemComm* **2013**, *4*, 112−119.
(48) Stahl, M. Modifications of the scoring function in FlexX for virtual screening applications. *Perspect. Drug Discovery Des.* **2000**, *20*, 83−98.
(49) Lin, C. M.; Hamel, E. Effects of inhibitors of tubulin polymerization on GTP hydrolysis. *J. Biol. Chem.* **1981**, *256*, 9242−9245.
(50) Mayer, M.; Meyer, B. Group epitope mapping by saturation transfer difference NMR to identify segments of a ligand in direct contact with a protein receptor. *J. Am. Chem. Soc.* **2001**, *123*, 6108−6117.
(51) Scheffers, D. J.; den Blaauwen, T.; Driessen, A. J. Non-hydrolysable GTP-gamma-S stabilizes the FtsZ polymer in a GDP-bound state. *Mol. Microbiol.* **2000**, *35*, 1211−1219.
(52) Urbina, J. A.; Concepcion, J. L.; Caldera, A.; Payares, G.; Sanoja, C.; Otomo, T.; Hiyoshi, H. In vitro and in vivo activities of E5700 and ER-119884, two novel orally active squalene synthase inhibitors, against *Trypanosoma cruzi*. *Antimicrob. Agents Chemother.* **2004**, *48*, 2379−2387.
(53) Shaffer, C. L.; Gunduz, M.; Scialis, R. J.; Fang, A. F. Metabolism and disposition of a selective $\alpha_7$ nicotinic acetylcholine receptor agonist in humans. *Drug Metab. Dispos.* **2007**, *35*, 1188−1195.
(54) Bucher, C.; Sparr, C.; Schweizer, W. B.; Gilmour, R. Fluorinated quinine alkaloids: synthesis, X-ray structure analysis and antimalarial parasite chemotherapy. *Chem.—Eur. J.* **2009**, *15*, 7637−7647.